General Field Theory Treatment of *E*-Plane Waveguide Junction Circulators—Part II: Two-Disk Ferrite Configuration

M. EZZAT EL-SHANDWILY, MEMBER, IEEE, AHMAD A. KAMAL, MEMBER, IEEE, AND ESMAT A. F. ABDALLAH

Abstract—**This paper presents an analysis of the two-disk ferrite *E*-plane waveguide junction circulator as a boundary value problem. The junction is divided into different regions and the electromagnetic fields are obtained in each region. Matching of the fields at the common boundaries is used to obtain the characteristic modes in the ferrite–dielectric region. Point matching technique, at an imaginary boundary chosen between the center region of the junction and the waveguides, is used to obtain the circulator characteristics.**

Measurements carried out show good agreement between theory and experiment.

I. Introduction

IN THE *E*-PLANE junction circulator, the ferrite material may take the shape of a full height cylindrical rod. However, the longitudinal RF magnetic field, on which this type of circulator depends, is zero at the midheight of the junction and therefore, the center portion of the ferrite rod is not magnetically active. In addition, dielectric losses will be present in this central portion due to the large electric field which exists there. Thus the ferrite material may take the shape of two disks placed on the common walls of the waveguides, as shown in Fig. 1(a) and (b), where the longitudinal RF magnetic field is maximum. In this case a smaller volume of ferrite material than both cases of *H*-plane configuration and full height *E*-plane configuration is used.

For the purpose of the analysis in this paper, the central portion of the junction is divided into three regions which are: the lower ferrite disk, the dielectric material, and the upper ferrite disk, Fig. 1(a). The air surrounding the ferrite is considered to be region 4, while the waveguides are considered to be region 5, Fig. 1(b). Excitation takes place by the dominant TE_{10} mode via only one of the waveguides. Since the incident field varies along the z direction, and since the ferrite construction is not continuous along this direction, all the TE_{pq} and TM_{pq} waveguide modes are excited.

By setting up the boundary conditions at all the discontinuity surfaces, namely, the planes $z = h_1$, $z = (a - h_2)$, the cylindrical surface $r = R$, and performing the numerical matching of the fields at an imaginary boundary between region 4 and the waveguides (region 5), a system of nonhomogeneous linear equations determining the reflection coefficient, insertion loss, and isolation is found.

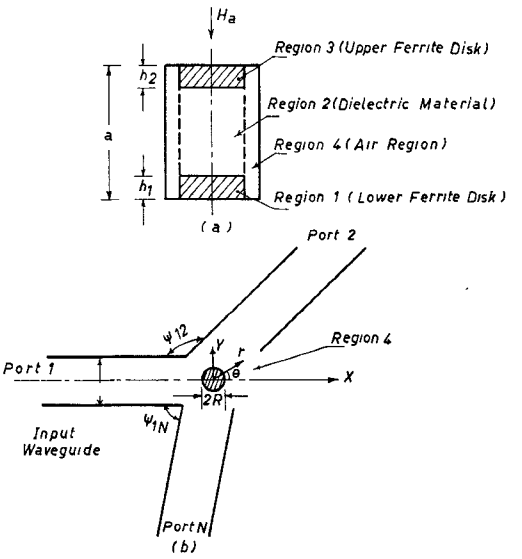

Fig. 1. (a) Schematic representation of the center portion of the two-disk ferrite *E*-plane junction circulator. (b) Plan view of the *N*-port two-ferrite disk *E*-plane circulator.

The same assumptions stated in the case of the full height ferrite configuration are also adopted during this analysis.

II. Theoretical Analysis of N-Port Circulators

In the published literature concerning propagation in a longitudinally magnetized ferrite structure, the discontinuity takes place in the radial direction (transverse to the direction of propagation). The propagation constants are determined from the simultaneous solution of the determinantal equation (obtained from application of boundary conditions) and the dispersion relation (obtained from the condition of consistency of solutions of the wave equations) [1], [2].

In the present problem, discontinuities take place along the direction of propagation, at the planes $z = h_1$ and $z = (a - h_2)$. Matching of the fields takes place along planes normal to the direction of propagation. This necessitates a new approach to the solution of the boundary value problem.

Maxwell's equations in the ferrite medium are

$$\nabla \times \bar{E} = -j\omega\mu_0[\mu] \cdot \bar{H} \tag{1}$$

$$\nabla \times \bar{H} = j\omega\varepsilon_0\varepsilon_f\bar{E}. \tag{2}$$

Manuscript received January 29, 1976; revised October 12, 1976.

M. E. El-Shandwily was with the Electrical and Electronic Research Laboratory, National Research Center, Cairo, Egypt. He is now with the Electrical Engineering Department, University of Technology, Tal Mohammad, Baghdad, Iraq.

A. A. Kamal is with the Department of Electronic Engineering, Cairo University, Cairo, Egypt.

E. A. F. Abdallah is with the Electrical and Electronic Research Laboratory, National Research Center, Cairo, Egypt.

By separating the transverse and the longitudinal components of the fields and the curl operator in the above two equations, we obtain

$$-j\omega\mu_0 H_z \bar{a}_z = \nabla_t \times \bar{E}_t \tag{3}$$

$$-j\omega\mu_0[\mu]\cdot\bar{H}_t = \nabla_t \times \bar{a}_z E_z + \bar{a}_z \times \frac{\partial \bar{E}_t}{\partial z} \tag{4}$$

$$j\omega\varepsilon_0\varepsilon_f E_z \bar{a}_z = \nabla_t \times \bar{H}_t \tag{5}$$

$$j\omega\varepsilon_0\varepsilon_f \bar{E}_t = \nabla_t \times \bar{a}_z H_z + \bar{a}_z \times \frac{\partial \bar{H}_t}{\partial z} \tag{6}$$

where t denotes the transverse plane, and $\bar{a}_z$ denotes a unit vector in the longitudinal Z direction.

From (3) to (6), and after making some algebraic and vector manipulation we get the following two wave equations in the ferrite medium:

$$\frac{1}{\mu}\frac{\partial^2 H_z}{\partial z^2} + \nabla_t^2 H_z + \omega^2\varepsilon_0\varepsilon_f\mu_0 H_z + \omega\varepsilon_0\varepsilon_f\frac{K}{\mu}\frac{\partial E_z}{\partial z} = 0 \tag{7}$$

$$\nabla_t^2 E_z + \frac{\partial^2 E_z}{\partial z^2} - \frac{\omega\mu_0 K}{\mu}\frac{\partial H_z}{\partial z} + \omega^2\varepsilon_0\varepsilon_f\mu_e E_z = 0 \tag{8}$$

where

$$\mu_e = \text{effective permeability} = \frac{\mu^2 - K^2}{\mu}.$$

The second step is to obtain $\bar{H}_t$ and $\bar{E}_t$ in terms of the longitudinal components H_z and E_z and their derivatives. From (3) to (6) we get the following relations:

$$\begin{aligned}\omega^2\varepsilon_0\varepsilon_f\mu_0\mu_e\bar{H}_t + 2\frac{\partial^2\bar{H}_t}{\partial z^2} + \frac{1}{\omega^2\varepsilon_0\varepsilon_f\mu_0\mu}\frac{\partial^4\bar{H}_t}{\partial z^4} \\ = \frac{\omega\varepsilon_0\varepsilon_f K}{\mu}\nabla_t E_z - j\omega\varepsilon_0\varepsilon_f\bar{a}_z\times\nabla_t E_z \\ + \frac{1}{j\omega\mu_0\mu}\bar{a}_z\times\nabla_t\frac{\partial^2 E_z}{\partial z^2} + \nabla_t\frac{\partial H_z}{\partial z} \\ - \frac{K}{j\mu}\nabla_t\times\bar{a}_z\frac{\partial H_z}{\partial z} + \frac{1}{\omega^2\varepsilon_0\varepsilon_f\mu_0\mu}\nabla_t\frac{\partial^3 H_z}{\partial z^3}\end{aligned} \tag{9}$$

From (9) and (10) we obtain H_r, H_θ, E_r, and E_θ in terms of the longitudinal components and their derivatives.

Since we are going to match the field components on the lower ferrite disk–dielectric interface and on the dielectric–upper ferrite disk interface, i.e., at $z = h_1$ and $z = (a - h_2)$, we should assume the same transverse variation of the field components in the three regions 1, 2, and 3. Therefore, let

$$E_z = \xi_t Z, \qquad H_z = \xi_t Z' \tag{11}$$

where ξ_t is the field distribution in the transverse direction, Z and Z' are functions of z only. Substituting (11) into the wave equation we get

$$\frac{1}{\xi_t}\nabla_t^2\xi_t + \frac{1}{Z'\mu}\frac{d^2Z'}{dz^2} + K_f^2 + \frac{\omega\varepsilon_0\varepsilon_f K}{\mu Z'}\frac{dZ}{dz} = 0 \tag{12}$$

$$\frac{1}{\xi_t}\nabla_t^2\xi_t + \frac{1}{Z}\frac{d^2Z}{dz^2} + K_f^2\mu_e - \frac{\omega\mu_0 K}{\mu Z}\frac{dZ'}{dz} = 0 \tag{13}$$

where

$$K_f^2 = \omega^2\varepsilon_0\varepsilon_f\mu_0. \tag{14}$$

Assume

$$\frac{1}{\xi_t}\nabla_t^2\xi_t = -K_c^2$$

from which we obtain

$$\xi_t \propto J_n(K_c r)\exp(jn\theta). \tag{15}$$

Substituting (14) into (12) and (13), and eliminating Z' gives

$$\begin{aligned}\frac{d^4Z}{dz^4} + [2\mu K_f^2 - K_c^2(\mu+1)]\frac{d^2Z}{dz^2} \\ + \mu(K_f^2\mu_e - K_c^2)(K_f^2 - K_c^2)Z = 0.\end{aligned} \tag{16}$$

Assume Z to vary as $\exp(-j\beta z)$. Substitute into (16), from which we get the following dispersion relation for the propagation constant in the Z direction:

$$\beta_{1,2}^2 = \tfrac{1}{2}\{[2\mu K_f^2 - K_c^2(\mu+1)] \pm \sqrt{[2\mu K_f^2 - K_c^2(\mu+1)]^2 - 4\mu(K_f^2\mu_e - K_c^2)(K_f^2 - K_c^2)}\}. \tag{17}$$

$$\begin{aligned}\frac{\partial^4\bar{E}_t}{\partial z^4} + 2\omega^2\varepsilon_0\varepsilon_f\mu_0\mu\frac{\partial^2\bar{E}_t}{\partial z^2} + (\omega^2\varepsilon_0\varepsilon_f\mu_0)^2(\mu^2 - K^2)\bar{E}_t \\ = \omega^2\varepsilon_0\varepsilon_f\mu_0\mu\nabla_t\frac{\partial E_z}{\partial z} + \nabla_t\frac{\partial^3 E_z}{\partial z^3} \\ + jK\omega^2\varepsilon_0\varepsilon_f\mu_0\nabla_t\times\bar{a}_z\frac{\partial E_z}{\partial z} + \omega\mu_0 K\nabla_t\frac{\partial^2 H_z}{\partial z^2} \\ + j\omega^3\mu_0^2\varepsilon_0\varepsilon_f(\mu^2 - K^2)\bar{a}_z\times\nabla_t H_z \\ + j\omega\mu_0\mu\bar{a}_z\times\nabla_t\frac{\partial^2 H_z}{\partial z^2}.\end{aligned} \tag{10}$$

We can now write

$$Z = A_1 e^{-j\beta_1 z} + A_2 e^{j\beta_1 z} + A_3 e^{-j\beta_2 z} + A_4 e^{j\beta_2 z} \tag{18}$$

$$Z' = g_1(-A_1 e^{-j\beta_1 z} + A_2 e^{j\beta_1 z}) + g_2(-A_3 e^{-j\beta_2 z} + A_4 e^{j\beta_2 z}) \tag{19}$$

where

$$g_{1,2} = \frac{j}{\omega\mu_0 K\beta_{1,2}}(K_c^2 + \beta_{1,2}^2 - \mu_e K_f^2).$$

For the lower ferrite disk (region 1) the tangential electric field components at $z = 0$ are zero. Using these boundary

conditions we get the following results:

$$A_1 = A_2 \quad \text{and} \quad A_3 = A_4$$

and therefore

$$E_z|_1 = \sum_{n=-\infty}^{\infty} J_n(K_c r)[A_{n1} \cos \beta_1 z + A_{n3} \cos \beta_2 z] \exp(jn\theta) \tag{20}$$

$$H_z|_1 = j \sum_{n=-\infty}^{\infty} J_n(K_c r)[g_1 A_{n1} \sin \beta_1 z + g_2 A_{n3} \sin \beta_2 z] \exp(jn\theta) \tag{21}$$

$$E_r|_1 = -j \sum_{n=-\infty}^{\infty} \Big\{ K_c J_n'(K_c r)[(P_1 - g_1 R_1)A_{n1} \sin \beta_1 z + (P_2 - g_2 R_2)A_{n3} \sin \beta_2 z] + \frac{jn}{r} J_n(K_c r)[(Q_1 - g_1 S_1)A_{n1} \sin \beta_1 z + (Q_2 - g_2 S_2)A_{n3} \sin \beta_2 z] \Big\} \exp(jn\theta) \tag{22}$$

$$E_\theta|_1 = -j \sum_{n=-\infty}^{\infty} \Big\{ K_c J_n'(K_c r)[(g_1 S_1 - Q_1)A_{n1} \sin \beta_1 z + (g_2 S_2 - Q_2)A_{n3} \sin \beta_2 z] + \frac{jn}{r} J_n(K_c r)[(P_1 - g_1 R_1)A_{n1} \sin \beta_1 z + (P_2 - g_2 R_2)A_{n3} \sin \beta_2 z] \Big\} \cdot \exp(jn\theta) \tag{23}$$

$$H_r|_1 = \sum_{n=-\infty}^{\infty} \Big\{ K_c J_n'(K_c r)[(T_1 - g_1 P_1)A_{n1} \cos \beta_1 z + (T_2 - g_2 P_2)A_{n3} \cos \beta_2 z] + \frac{jn}{r} J_n(K_c r)[(U_1 - g_1 Q_1)A_{n1} \cos \beta_1 z + (U_2 - g_2 Q_2)A_{n3} \cos \beta_2 z] \Big\} \exp(jn\theta) \tag{24}$$

$$H_\theta|_1 = \sum_{n=-\infty}^{\infty} \Big\{ K_c J_n'(K_c r)[(g_1 Q_1 - U_1)A_{n1} \cos \beta_1 z + (g_2 Q_2 - U_2)A_{n3} \cos \beta_2 z] + \frac{jn}{r} J_n(K_c r)[(T_1 - g_1 P_1)A_{n1} \cos \beta_1 z + (T_2 - g_2 P_2)A_{n3} \cos \beta_2 z] \Big\} \exp(jn\theta). \tag{25}$$

For the upper ferrite disk (region 3), and when using the boundary condition

$$E_r|_3 = E_\theta|_3 = 0, \qquad \text{at } z = a \tag{26}$$

we get a field distribution similar to (20)–(25), except that A_{n1} is replaced by C_{n1}, A_{n3} by C_{n3}, $\beta_1 z$ by $\beta_1(z-a)$, and $\beta_2 z$ by $\beta_2(z-a)$, where

$$\begin{aligned}
P_i &= -j\beta_i(-\beta_i^2 + K_f^2\mu)/\Delta_i \\
Q_i &= \beta_i K_f^2 K/\Delta_i \\
R_i &= -\omega\mu_0 K\beta_i^2/\Delta_i \\
S_i &= -j\omega[-\mu_0\mu\beta_i^2 + K_f^2\mu_0(\mu^2 - K^2)]/\Delta_i \\
T_i &= \omega^3\varepsilon_0^2\varepsilon_f^2\mu_0 K/\Delta_i \\
U_i &= j\omega(-\varepsilon_0\varepsilon_f\beta_i^2 + \omega^2\varepsilon_0^2\varepsilon_f^2\mu_0\mu)/\Delta_i \\
\Delta_i &= [-\beta_i^2 + K_f^2(\mu + K)][-\beta_i^2 + K_f^2(\mu - K)]
\end{aligned}$$

and

$$i = 1,2.$$

For the dielectric medium, region 2, we put $K = 0, \varepsilon_f = \varepsilon_d$, and $\mu = 1$ in the previous equations to obtain the following field components:

$$E_z|_2 = \sum_{n=-\infty}^{\infty} J_n(K_c r)[B_{n1} \sin \beta_d z + B_{n2} \cos \beta_d z] \exp(jn\theta) \tag{27}$$

$$H_z|_2 = \sum_{n=-\infty}^{\infty} J_n(K_c r)[B_{n3} \sin \beta_d z + B_{n4} \cos \beta_d z] \exp(jn\theta) \tag{28}$$

$$E_r|_2 = \sum_{n=-\infty}^{\infty} \Big\{ \frac{\beta_d}{K_c} J_n'(K_c r)[B_{n1} \cos \beta_d z - B_{n2} \sin \beta_d z] - \frac{jn}{r} J_n(K_c r) \frac{j\omega\mu_0}{K_c^2} \cdot [B_{n3} \sin \beta_d z + B_{n4} \cos \beta_d z] \Big\} \exp(jn\theta) \tag{29}$$

$$E_\theta|_2 = \sum_{n=-\infty}^{\infty} \Big\{ \frac{jn}{r} J_n(K_c r) \frac{\beta_d}{K_c^2} [B_{n1} \cos \beta_d z - B_{n2} \sin \beta_d z] + \frac{j\omega\mu_0}{K_c} J_n'(K_c r) \cdot [B_{n3} \sin \beta_d z + B_{n4} \cos \beta_d z] \Big\} \exp(jn\theta) \tag{30}$$

$$H_r|_2 = \sum_{n=-\infty}^{\infty} \Big\{ \frac{jn}{r} J_n(K_c r) \frac{j\omega\varepsilon_0\varepsilon_d}{K_c^2} [B_{n1} \sin \beta_d z + B_{n2} \cos \beta_d z] + \frac{\beta_d}{K_c} J_n'(K_c r) \cdot [B_{n3} \cos \beta_d z - B_{n4} \sin \beta_d z] \Big\} \exp(jn\theta) \tag{31}$$

$$H_\theta|_2 = \sum_{n=-\infty}^{\infty} \left\{ -\frac{j\omega\varepsilon_0\varepsilon_d}{K_c}[B_{n1}\sin\beta_d z + B_{n2}\cos\beta_d z] + \frac{jn}{r}J_n(K_c r)\frac{\beta_d}{K_c^2} \cdot [B_{n3}\cos\beta_d z - B_{n4}\sin\beta_d z] \right\} \exp(jn\theta) \quad (32)$$

where

$$\beta_d^2 = K_d^2 - K_c^2. \quad (33)$$

The continuity of the tangential electric and magnetic field components at the interface between regions 1 and 2 is used to determine the constants B_{n1}, B_{n2}, B_{n3}, and B_{n4} in terms of A_{n1} and A_{n3}. The result can be arranged such that each B_n is given in terms of A_{n1} and A_{n3}. Also, the continuity of the tangential electric and magnetic field components at the interface between regions 3 and 2 gives four equations, each involving one of the B_n's in terms of C_{n1} and C_{n3}. The resulting expressions are long, and will not be written here. Now, B_{ni} ($i = 1, 2, 3,$ and 4), which is obtained from the first set of equations, is equated to the corresponding B_{ni} which is obtained from the second set of equations. The result is a set of four homogeneous equations in A_{n1}, A_{n3}, C_{n1}, and C_{n3}.

In order to have a solution, the determinant of their coefficient should equal to zero. This determinantal equation is a function only of K_c^2. For any value of frequency, ferrite and dielectric materials, we have an infinite set of values of K_c^2 that satisfy this equation. Once each of the values of K_c^2 is substituted in the dispersion relation (17) we obtain the propagation constants β_1 and β_2 in the ferrite material and in (33) to get β_d in the dielectric material.

The four homogeneous equations in the complex amplitudes A_{n1}, A_{n3}, C_{n1}, and C_{n3} may be written in a compact form as follows:

$$\begin{aligned} a_{11}A_{n1} + a_{12}A_{n3} + a_{13}C_{n1} + a_{14}C_{n3} &= 0 \\ a_{21}A_{n1} + a_{22}A_{n3} + a_{23}C_{n1} + a_{24}C_{n3} &= 0 \\ a_{31}A_{n1} + a_{32}A_{n3} + a_{33}C_{n1} + a_{34}C_{n3} &= 0 \\ a_{41}A_{n1} + a_{42}A_{n3} + a_{43}C_{n1} + a_{44}C_{n3} &= 0 \end{aligned} \quad (34)$$

where $a_{11}, a_{12}, \cdots$, etc., are the elements of the determinant. When solving (34) simultaneously, A_{n3}, C_{n1}, and C_{n3} are found in terms of A_{n1}. The results are

$$A_{n3} = A_{n1}\frac{-a_{11}(a_{23}a_{34} - a_{24}a_{33}) + a_{21}(a_{13}a_{34} - a_{14}a_{33}) - a_{31}(a_{13}a_{24} - a_{14}a_{23})}{a_{12}(a_{23}a_{34} - a_{24}a_{33}) - a_{22}(a_{13}a_{34} - a_{14}a_{33}) + a_{32}(a_{13}a_{24} - a_{14}a_{23})} = MA_{n1} \quad (35)$$

$$C_{n1} = A_{n1}\frac{(a_{24}a_{11} - a_{14}a_{21}) + (a_{24}a_{12} - a_{14}a_{22})M}{(a_{14}a_{23} - a_{24}a_{13})} = W_5 A_{n1} \quad (36)$$

$$C_{n3} = -A_{n1}\frac{a_{11} + a_{13}W_5 + a_{12}M}{a_{14}} = W_6 A_{n1}. \quad (37)$$

Substituting (35) into the values of $B_{n1}, \cdots, B_{n4}$ we get the following:

$$B_{n1} = (a_{11} + Ma_{12})A_{n1} = W_1 A_{n1} \quad (38)$$

$$B_{n2} = (a_{21} + Ma_{22})A_{n1} = W_2 A_{n1} \quad (39)$$

$$B_{n3} = (a_{31} + Ma_{32})A_{n1} = W_3 A_{n1} \quad (40)$$

$$B_{n4} = (a_{41} + Ma_{42})A_{n1} = W_4 A_{n1}. \quad (41)$$

For the field distribution in the air surrounding the ferrite–dielectric structure, region 4, it is written as in Part I,[1] (10)–(13).

The second step in the analysis is to get the complex amplitudes $F_{m,n1}$, $F_{m,n2}$, $H_{m,n1}$, and $H_{m,n2}$ in terms of A_{n1} only. This is done by the use of the continuity conditions of the tangential electromagnetic field components on the boundary between region 4 from one side and regions 1–3 on the other side, i.e., on the cylindrical surface $r = R$. Take E_z as an example

$$\begin{aligned} E_z(R,\theta,z)|_4 &= E_z(R,\theta,z)|_1, && 0 \le z \le h_1 \\ &= E_z(R,\theta,z)|_2, && h_1 \le z \le (a - h_2) \\ &= E_z(R,\theta,z)|_3, && (a - h_2) \le z \le a. \end{aligned} \quad (42)$$

These boundary conditions are applicable in the range of θ from 0 to 2π, and therefore, the summation on n in the expressions of E_z in (42) can be eliminated, due to the orthogonality properties of the exponential functions.

By multiplying (42) by $\cos(l\pi z/a)$ and integrating from $z = 0$ to $z = a$, we obtain the following:

$$F_{l,n1}J_n(K_a R) + F_{l,n2}Y_n(K_a R) = \sum_{i=1}^{\infty} L_{1i}A_{n1i} \quad (43)$$

where

$$L_{1i} = \frac{2}{a}[I_1 + MI_2 + W_1 I_3 + W_2 I_4 + W_5 I_5 + W_6 I_6]J_n(K_{ci}R)$$

$$I_1 = \frac{\beta_4 \sin\beta_4 h_1 \cos\beta_1 h_1 - \beta_1 \cos\beta_4 h_1 \sin\beta_1 h_1}{\beta_4^2 - \beta_1^2}$$

$$I_2 = (\beta_4 \sin\beta_4 h_1 \cos\beta_2 h_1 - \beta_2 \cos\beta_4 h_1 \sin\beta_2 h_1)/(\beta_4^2 - \beta_2^2)$$

$$I_3 = [\beta_d \cos\beta_d h_1 \cos\beta_4 h_1 + \beta_4 \sin\beta_d h_1 \sin\beta_4 h_1 - \beta_d \cos\beta_d(a - h_2)\cos\beta_4(a - h_2) - \beta_4 \sin\beta_d(a - h_2)\sin\beta_4(a - h_2)]/(\beta_d^2 - \beta_4^2)$$

$$I_4 = [\beta_4 \sin\beta_d(a - h_2)\cos\beta_4(a - h_2) - \beta_d \cos\beta_d(a - h_2)\sin\beta_4(a - h_2) - \beta_4 \sin\beta_d h_1 \cdot \cos\beta_4 h_1 + \beta_d \cos\beta_d h_1 \sin\beta_4 h_1]/(\beta_4^2 - \beta_d^2)$$

[1] See Part I of this paper, pp. 782–791 of this issue.

$$I_5 = [-\beta_4 \sin \beta_4(a-h_2)\cos \beta_1 h_2 - \beta_1 \cos \beta_4(a-h_2)\sin \beta_1 h_2]/(\beta_4^2-\beta_1^2)$$

$$I_6 = [-\beta_4 \sin \beta_4(a-h_2)\cos \beta_2 h_2 - \beta_2 \cos \beta_4(a-h_2)\sin \beta_2 h_2]/(\beta_4^2-\beta_2^2)$$

$$\beta_4 = l\pi/a.$$

Applying the same technique to the other three boundary conditions of H_z, E_θ, and H_θ, we obtain the following three equations:

$$H_{l,n1}J_n(K_aR) + H_{l,n2}Y_n(K_aR) = \sum_{i=1}^{\infty} L_{2i}A_{n1i} \quad (44)$$

$$e_{n1}F_{l,n1} + e_{n2}F_{l,n2} - d_{n1}H_{l,n1} - d_{n2}H_{l,n2} = \sum_{i=1}^{\infty} L_{3i}A_{n1i} \quad (45)$$

$$-f_{n1}F_{l,n1} - f_{n2}F_{l,n2} + e_{n1}H_{l,n1} + e_{n2}H_{l,n2} = \sum_{i=1}^{\infty} L_{4i}A_{n1i} \quad (46)$$

where

$$L_{2i} = \frac{2}{a}[-g_1 I_7 - g_2 M I_8 + jW_3 I_9 + jW_4 I_{10} - g_1 W_5 I_{11} - g_2 W_6 I_{12}]J_n(K_{ci}R)$$

$$L_{3i} = \frac{2}{a}\Big\{K_{ci}J_n'(K_{ci}R)[(S_1 g_1 - Q_1)(I_7 + W_5 I_{11}) + (S_2 g_2 - Q_2)(MI_8 + W_6 I_{12})] + \frac{jn}{R}J_n(K_{ci}R)[(P_1 - g_1 R_1)(I_7 + W_5 I_{11}) + (P_2 - g_2 R_2)(MI_8 + W_6 I_{12})] - \left[\frac{n}{R}\frac{\beta_{di}^2}{K_{ci}^2}J_n(K_{ci}R)(W_1 I_{10} - W_2 I_9) + \frac{\omega\mu_0}{K_{ci}}J_n(K_{ci}R)(W_3 I_9 + W_4 I_{10})\right]\Big\}$$

$$L_{4i} = \frac{2}{a}\Big\{K_{ci}J_n'(K_{ci}R)[(Q_1 g_1 - U_1)(I_1 + W_5 I_5) + (Q_2 g_2 - U_2)(MI_2 + W_6 I_6)] + \frac{jn}{R}J_n(K_{ci}R)[(T_1 - P_1 g_1)(I_1 + W_5 I_5) + (T_2 - P_2 g_2)(MI_2 + W_6 I_6)] - \frac{j\omega\varepsilon_0\varepsilon_d}{K_{ci}}J_n'(K_{ci}R)(W_1 I_3 + W_2 I_4) + \frac{jn}{R}J_n(K_{ci}R)\frac{\beta_d}{K_{ci}^2}(W_3 I_4 - W_4 I_3)\Big\}$$

$$e_{n1} = \frac{jnG_a}{R}J_n(K_aR)$$

$$e_{n2} = \frac{jnG_a}{R}Y_n(K_aR)$$

$$f_{n1} = U_a K_a J_n'(K_aR)$$

$$f_{n2} = U_a K_a Y_n'(K_aR)$$

$$d_{n1} = S_a K_a J_n'(K_aR)$$

$$d_{n2} = S_a K_a Y_n'(K_aR)$$

$$I_7 = (-\beta_4 \cos \beta_4 h_1 \cos \beta_1 h_1 + \beta_1 \sin \beta_4 h_1 \cos \beta_1 h_1)/(\beta_4^2-\beta_1^2)$$

$$I_8 = (-\beta_4 \cos \beta_4 h_2 \cos \beta_2 h_1 + \beta_2 \sin \beta_4 h_1 \cos \beta_2 h_1)/(\beta_4^2-\beta_2^2)$$

$$I_9 = [-\beta_4 \cos \beta_4(a-h_2)\sin \beta_d(a-h_2) + \beta_d \sin \beta_4(a-h_2)\cos \beta_d(a-h_2) + \beta_4 \cos \beta_4 h_1 \sin \beta_d h_1 - \beta_d \sin \beta_4 h_1 \cos \beta_d h_1]/(\beta_4^2-\beta_d^2)$$

$$I_{10} = [\beta_4 \cos \beta_4 h_1 \cos \beta_d h_1 + \beta_d \sin \beta_4 h_1 \sin \beta_d h_1 - \beta_4 \cos \beta_4(a-h_2)\cos \beta_d(a-h_2) - \beta_d \sin \beta_4(a-h_2)\sin \beta_d(a-h_2)]/(\beta_4^2-\beta_d^2)$$

$$I_{11} = [-\beta_4 \cos \beta_4(a-h_2)\sin \beta_1 h_2 - \beta_1 \sin \beta_4(a-h_2)\cos \beta_1 h_2]/(\beta_4^2-\beta_1^2)$$

$$I_{12} = [-\beta_4 \cos \beta_4(a-h_2)\sin \beta_2 h_2 - \beta_2 \sin \beta_4(a-h_2)\cos \beta_2 h_2]/(\beta_4^2-\beta_2^2)$$

$$\beta_4 = l\pi/a.$$

Equations (43)–(46) are four equations in the unknowns $F_{l,n1}$, $F_{l,n2}$, $H_{l,n1}$, and $H_{l,n2}$. When solving these equations, these complex amplitudes are determined in terms of an infinite summation on A_{n1i}. The result takes the following form:

$$F_{l,n1} = \sigma_4 \sum_{i=1}^{\infty}\Omega_{1i}A_{n1i} + \sigma_5 \sum_{i=1}^{\infty}\Omega_{2i}A_{n1i} = \sum_{i=1}^{\infty}F_{11}A_{n1i} \quad (47)$$

$$H_{l,n1} = \sigma_6 \sum_{i=1}^{\infty}\Omega_{1i}A_{n1i} + \sigma_4 \sum_{i=1}^{\infty}\Omega_{2i}A_{n1i} = \sum_{i=1}^{\infty}H_{11}A_{n1i} \quad (48)$$

$$F_{l,n2} = \frac{1}{Y_n(K_aR)}\sum_{i=1}^{\infty}[L_{1i} - \sigma_4\Omega_{1i}J_n(K_aR) - \sigma_5\Omega_{2i}J_n(K_aR)]A_{n1i} = \sum_{i=1}^{\infty}F_{22}A_{n1i} \quad (49)$$

$$H_{l,n2} = \frac{1}{Y_n(K_aR)}\sum_{i=1}^{\infty}[L_{2i} - \sigma_6\Omega_{1i}J_n(K_aR) - \sigma_4\Omega_{2i}J_n(K_aR)]A_{n1i} = \sum_{i=1}^{\infty}H_{22}A_{n1i} \quad (50)$$

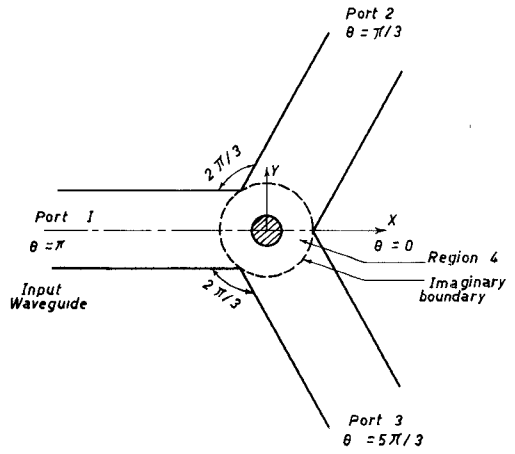

Fig. 2. Schematic representation of the Y-type two-disk *E*-plane circulator.

where

$$\sigma_4 = \sigma_1/(\sigma_1^2 - \sigma_2\sigma_3)$$
$$\sigma_5 = \sigma_2/(\sigma_1^2 - \sigma_2\sigma_3)$$
$$\sigma_6 = \sigma_3/(\sigma_1^2 - \sigma_2\sigma_3)$$
$$\sigma_1 = e_{n1} - e_{n2}J_n(K_aR)/Y_n(K_aR)$$
$$\sigma_2 = d_{n1} - d_{n2}J_n(K_aR)/Y_n(K_aR)$$
$$\sigma_3 = f_{n1} - f_{n2}J_n(K_aR)/Y_n(K_aR)$$
$$\Omega_{1i} = L_{3i} - \frac{L_{1i}e_{n2}}{Y_n(K_aR)} + \frac{L_{2i}d_{n2}}{Y_n(K_aR)}$$
$$\Omega_{2i} = L_{4i} - \frac{L_{1i}f_{n2}}{Y_n(K_aR)} + \frac{L_{2i}e_{n2}}{Y_n(K_aR)}$$
$$F_{11} = \sigma_4\Omega_{1i} + \sigma_5\Omega_{2i}$$
$$H_{11} = \sigma_6\Omega_{1i} + \sigma_4\Omega_{2i}$$
$$F_{22} = \frac{1}{Y_n(K_aR)}[L_{1i} - \sigma_4\Omega_{1i}J_n(K_aR) - \sigma_5\Omega_{2i}J_n(K_aR)]$$
$$H_{22} = \frac{1}{Y_n(K_aR)}[L_{2i} - \sigma_6\Omega_{1i}J_n(K_aR) - \sigma_4\Omega_{2i}J_n(K_aR)].$$

The electromagnetic field components in the waveguides have been written in Part I,[1] (14)–(28). These field distributions are also applicable in this case, so they will not be repeated here for the sake of briefness.

Until now, the analysis is general and may be applied to any junction with any number of ports whether symmetrical or nonsymmetrical. In order to get numerical results, we shall use the Y-junction circulator as an example.

A. The Two-Disk Y-Junction Circulator

The imaginary wall between region 4 and the three waveguides (region 5) is chosen to be a cylindrical wall as in the case of the full height Y-junction circulator, Part I.[1] The axis of this cylindrical surface coincides with the junction axis and its radius is $b/\sqrt{3}$ as shown in Fig. 2. Same boundary conditions on this imaginary boundary (29)–(32) in Part I[1] are also applicable in this case. For the case of the input waveguide ($i = 1$), substitute in these boundary conditions by the field distributions in region 4 and in the input waveguide using the relations (47)–(50). When using the orthogonality properties of the trigonometric functions, we get the following set of equations:

$$\sum_{n=-\infty}^{\infty}\sum_{i=1}^{\infty}\left[F_{11}J_n\left(K_a\frac{b}{\sqrt{3}}\right) + F_{22}Y_n\left(K_a\frac{b}{\sqrt{3}}\right)\right]A_{n1i}\exp(jn\theta) + \sum_{q=0}^{\infty}\left[\frac{-j\omega\mu_0}{\Gamma_{lq}}b_{lq}\frac{q\pi}{b}\sin q\pi\left(\frac{\sin\theta}{\sqrt{3}}+\frac{1}{2}\right) + a_{lq}\frac{l\pi}{a}\sin q\pi\left(\frac{\sin\theta}{\sqrt{3}}+\frac{1}{2}\right)\right]\cdot\exp(\Gamma_{lq}b\cos\theta/\sqrt{3}) = 0, \quad l = 0, 1, 2, \cdots, \infty \quad (51)$$

$$j\sum_{n=-\infty}^{\infty}\sum_{i=1}^{\infty}\left[H_{11}J_n\left(K_a\frac{b}{\sqrt{3}}\right) + H_{22}Y_n\left(K_a\frac{b}{\sqrt{3}}\right)\right]A_{n1i}\exp(jn\theta) + \sum_{q=0}^{\infty}\left[j\omega\varepsilon_0\frac{a_{lq}}{\Gamma_{lq}}\frac{q\pi}{b}\cos q\pi(\sin\theta/\sqrt{3}+\tfrac{1}{2}) + \frac{l\pi}{a}b_{lq}\cos q\pi\left(\frac{\sin\theta}{\sqrt{3}}+\frac{1}{2}\right)\right]\exp(\Gamma_{lq}b\cos\theta/\sqrt{3}) = \delta_{1l}\left[-\frac{\pi}{a}\exp(-jK_db\cos\theta/\sqrt{3})\right], \quad l = 1, 2, \cdots, \infty \quad (52)$$

$$-j\sum_{n=-\infty}^{\infty}\sum_{i=1}^{\infty}[F_{11}e_{n3} + F_{22}e_{n4} - H_{11}d_{n3} - H_{22}d_{n4}]A_{n1i}\exp(jn\theta) + \sum_{q=0}^{\infty}\left[a_{lq}\frac{q\pi}{b}\cos q\pi\left(\frac{\sin\theta}{\sqrt{3}}+\frac{1}{2}\right)\cos\theta - \frac{a_{lq}}{\Gamma_{lq}}K_{lq}^2\sin q\pi\left(\frac{\sin\theta}{\sqrt{3}}+\frac{1}{2}\right)\sin\theta + \frac{j\omega\mu_0}{\Gamma_{lq}}b_{lq}\frac{l\pi}{a}\cos q\pi\left(\frac{\sin\theta}{\sqrt{3}}+\frac{1}{2}\right)\cos\theta\right]\cdot\exp(\Gamma_{lq}b\cos\theta/\sqrt{3}) = \delta_{1l}\left[\frac{\omega\mu_0}{K_d}\frac{\pi}{a}\cos\theta\exp(-jK_db\cos\theta/\sqrt{3})\right], \quad l = 1, 2, \cdots, \infty \quad (53)$$

$$\sum_{n=-\infty}^{\infty}\sum_{i=1}^{\infty}[-F_{11}f_{n3}-F_{22}f_{n4}+H_{11}e_{n3}+H_{22}e_{n4}]A_{n1i}\exp(jn\theta)$$
$$-\sum_{q=0}^{\infty}\left[-j\omega\varepsilon_0\frac{a_{lq}}{\Gamma_{lq}}\frac{l\pi}{a}\sin q\pi\left(\frac{\sin\theta}{\sqrt{3}}+\frac{1}{2}\right)\cdot\cos\theta+\frac{q\pi}{b}b_{lq}\sin q\pi\left(\frac{\sin\theta}{\sqrt{3}}+\frac{1}{2}\right)\cdot\cos\theta+b_{lq}\frac{K_{lq}^2}{\Gamma_{lq}}\cos q\pi\left(\frac{\sin\theta}{\sqrt{3}}+\frac{1}{2}\right)\sin\theta\right]\cdot\exp(\Gamma_{lq}b\cos\theta/\sqrt{3})$$
$$=\delta_{1l}\left[\frac{jK_{10}^2}{K_d}\sin\theta\exp(-jK_db\cos\theta/\sqrt{3})\right],\qquad l=0,1,2,\cdots,\infty \quad (54)$$

where

$$e_{n3}=\frac{jnG_a}{b/\sqrt{3}}J_n\left(K_a\frac{b}{\sqrt{3}}\right)$$
$$e_{n4}=\frac{jnG_a}{b/\sqrt{3}}Y_n\left(K_a\frac{b}{\sqrt{3}}\right)$$
$$d_{n3}=S_aK_aJ_n'\left(K_a\frac{b}{\sqrt{3}}\right)$$
$$d_{n4}=S_aK_aY_n'\left(K_a\frac{b}{\sqrt{3}}\right)$$
$$f_{n3}=U_aK_aJ_n'\left(K_a\frac{b}{\sqrt{3}}\right)$$
$$f_{n4}=U_aK_aY_n'\left(K_a\frac{b}{\sqrt{3}}\right).$$

δ_{1l}, Γ_{lq}, K_{lq}, K_d, and K_{10} are as defined before in Part I.[1]

Replacing a_{lq} by a'_{lq}, b_{lq} by b'_{lq}, θ by $(\theta+2\pi/3)$, and equating the right-hand side of (51)–(54) to zero, we get a set of four homogeneous equations corresponding to waveguide 2. Similar equations are derived in waveguide 3, by replacing a_{lq} by a''_{lq}, b_{lq} by b''_{lq}, θ by $(\theta+4\pi/3)$ in the same equations, and also equating the right-hand side to zero, since there are no incident waves on ports 2 and 3.

In order to obtain the circulator characteristics, we use the point matching technique on the imaginary boundary between regions 4 and 5. Truncation in the seven infinite unknowns should be done. Also, a finite value for l should be chosen. Consider N cylindrical modes, Q_1 transverse electric modes, Q_2 transverse magnetic modes, and $i=1,2,\cdots,M$, i.e., we have M roots for the determinantal equation. For $l=0,1,\cdots,L$, all TE_{lq} and TM_{lq}, up to TE_{LQ_1} and TM_{LQ_2} are excited. For p matching points in each waveguide, we have the following:

total number of equations $=6p(2L+1)$;
number of cylindrical complex amplitudes $=M(2N+1)$;
number of TE complex amplitudes $=3[L(Q_1+1)+Q_1]$;
number of TM complex amplitudes $=3LQ_2$.

In order to have a solution, the total number of equations should be equal to the number of unknowns, therefore

$$6p(2L+1)=M(2N+1)+3[L(Q_1+1)+Q_1]+3LQ_2. \quad (55)$$

III. Numerical and Experimental Results

The numerical solution consists of two main parts, the results of one part are considered the necessary data to the other. These two parts are

i) the determination of K_c, and consequently the propagation constants in each of regions 1, 2, and 3;
ii) the determination of the circulator characteristics, numerically.

The determinantal equation is solved numerically using the false position method up to the accuracy of 10^{-8}. The pivoting method of Gauss is used to numerically solve the simultaneous linear equations to obtain the waveguide mode amplitudes, the cylindrical mode amplitudes, and consequently the circulator characteristics.

In order to check the correctness of the results, a case very near to the full height case is first chosen. This case is $h_1=h_2=0.4$ in ($a=0.9$ in) and the permittivity of the dielectric region (region 2) is taken equal to the ferrite permittivity. Two cases have been calculated numerically for $R=0.1$ in using the first ferrite material (Y13A) over the entire X band and plotted together with the corresponding full height case in Fig. 3. It is clear from this figure that both the insertion loss and the isolation curves in the three cases are very close, while the reflection coefficient curves differ a little. By this method we are now sure of the validity of the analysis and the correctness of the program.

Many values for the propagation constants in each region have been obtained by solving the determinantal equation numerically, and the adopted solution needs only three values for the propagation constants in each region. So, it is important to study how the propagation constants are chosen. What is the most important root? What is the second root to be chosen, and what is the third root? The authors have studied this problem, and the conclusions are summarized as follows. From the analysis of Section II, we find that the denominators of the integrations $I_1, I_2, \cdots, I_{12}$ take the form of $[(l\pi/a)^2-\beta_1^2]$, or $[(l\pi/a)^2-\beta_2^2]$, or $[(l\pi/a)^2-\beta_d^2]$. In order to make $I_1, I_2, \cdots, I_{12}$ have effective values, these denominators should be as small as possible. This means that the values of β_1, β_2, and β_d which are near to $(l\pi/a)$, where l takes the values of 0 or 1, are the most important. Since the dominant mode (the most important mode) varies as π/a (137.793 rad/m) along the z direction, then the most important propagation constant is that nearest to the value π/a.

A. Numerical Results of the Propagation Constants

As it has been mentioned before, propagation constants are found from the solution of the dispersion relation together with the determinantal equation. There are infinite values of the solution that satisfy both relations at any frequency. These infinite roots represent the propagation

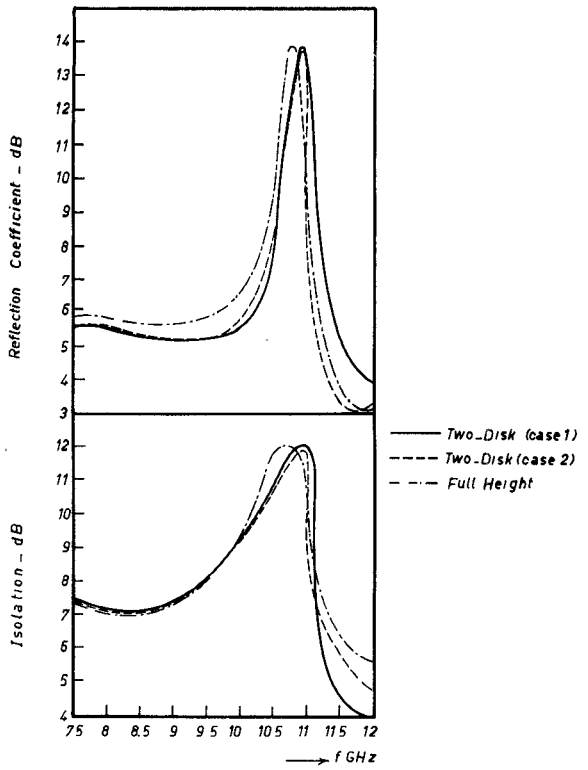

(a)

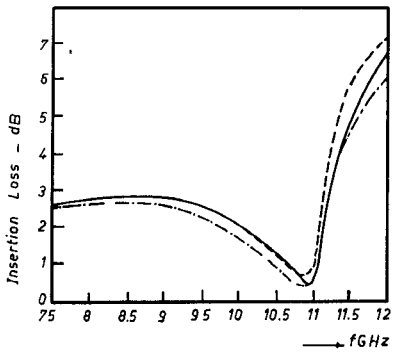

(b)

Fig. 3. Circulator characteristics for the full height and two-disk circulator, $R = 0.1$ in, $\varepsilon_d = \varepsilon_f$ (case 1: $P = 3$, $N = 4$, $Q_1 = 3$, $Q_2 = 2$, $M = 2$, $L = 1$; case 2: the same as case 1, but $L = 0.1$).

constants in each region. The propagation constants for different ferrite heights are calculated numerically and plotted against frequency. All calculations have been carried out for the ferrite material Y13A with $H_{dc} = 200$ Oe. Only sample calculations will be presented.

Fig. 4(a)–(c) shows a plot of frequency against β_1, β_2, and β_d when $h_1 = h_2 = 0.05$ in. It is clear from Fig. 4(a) and (b) that the frequency varies with β_1 and β_2 approximately in a linear manner. The values of β_1 and β_2 increase as the frequency increases and become larger, and larger than the value π/a. In this range of frequency β_1 and β_2 are always found to be real positive. As the frequency increases, we notice that the roots become near to each other until they reach very close values at the upper end of the frequency band (12.5 GHz). The values of β_2 are always smaller than the corresponding β_1 values. Since h_1 and h_2 are small compared with a, we find that the smallest values for β_1 and β_2 are 784.09 and 331.81 rad/m, respectively, which are very large compared to π/a. Fig. 4(c) shows a plot for the frequency versus β_d. It is clear from this figure that it consists of two groups, one of which has linear variation, while the second group is slightly curved, especially at the upper end of the frequency band. The values of β_d are very close to π/a when compared with the corresponding values of β_1 and β_2 in the ferrite material. β_d may have imaginary values which represent nonpropagating modes. β_d modes may be real positive, i.e., propagating, along the entire X band of frequency, may be real positive in the first part of the frequency range, and then transformed into an imaginary one (i.e., nonpropagating mode) in the rest of the frequency band, and may be imaginary all along the frequency band, with increasing values with frequency.

It is noticed from the numerical results obtained that when the ferrite disk is very small, the values of β_d are closer to π/a than the values of β_1 and β_2. When the ferrite disk height becomes large compared with the dielectric height we find that β_1 and β_2 become very near to π/a, while β_d takes larger values. These results are expected from physical considerations. When the ferrite disks are short, then the configuration is approximately similar to the full height dielectric rod and the effect of the ferrite is small. Therefore, the dielectric propagation constants are expected to be the dominant factors. In other words, those integrals from $I_1, I_2, \cdots, I_{12}$, which are related to the dielectric region, will be more important than the others. On the other side, when the ferrite disks are long, then the situation reverses and the ferrite propagation constants dominate.

In the next section, we shall use the calculated propagation constants to obtain the circulator characteristics for these ferrite disk heights for different ferrite radii.

B. Numerical and Experimental Results of Circulator Characteristics

Numerical results are obtained for the circulator characteristics when the disks height is 0.05 in and for different values of disk radii, and then these cases are verified experimentally. The numerical and experimental circulator characteristics for $R = 0.1$ in are shown in Fig. 5. It is noticed that the general shapes of the numerical and experimental results are nearly the same. Frequency of maximum isolation which is defined to be the frequency of circulation takes place numerically at 8.75 GHz, while it is found experimentally to be 8.85 GHz; this means that there is a shift in the frequency of circulation by only 0.10 GHz, and the value of isolation is slightly less. For frequencies equal to or larger than 9.25 GHz, most of the power is reflected back from the input port, and the power output from the other two ports is very small. It is clear from Fig. 5 that there is only one frequency of circulation, and no other circulation frequencies in the same or opposite sense of circulation have appeared. Comparing this result with the corresponding characteristics, for the full height case using the same ferrite material and radius, we find that removing the central portion of the ferrite rod decreases the circulation frequency

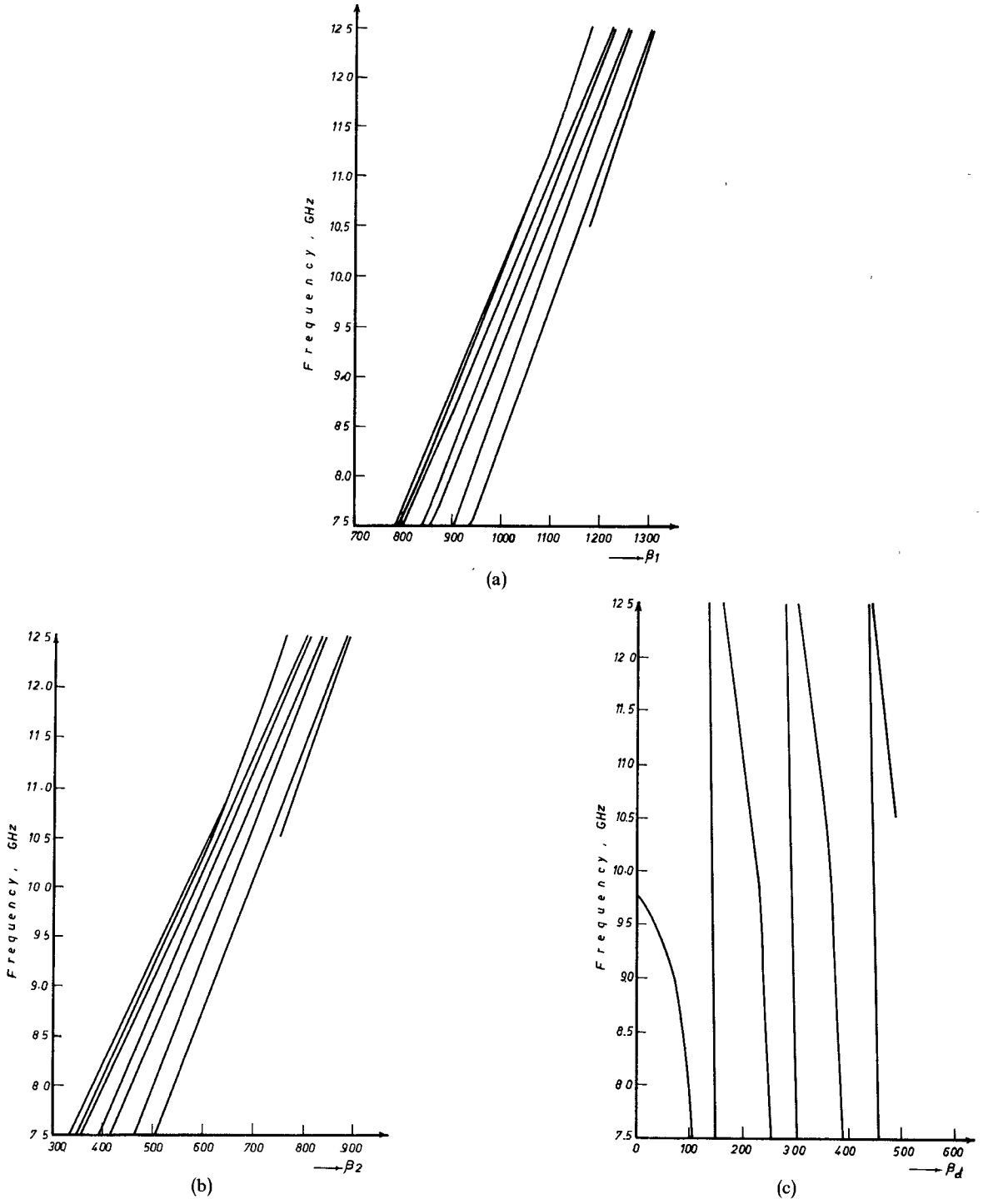

Fig. 4. (a) Frequency versus propagation constant β_1 in the two ferrite disks, $h_1 = h_2 = 0.05$ in, $\varepsilon_d = 1$. (b) Frequency versus propagation constant β_2 in the two ferrite disks, $h_1 = h_2 = 0.05$ in, $\varepsilon_d = 1$. (c) Frequency versus propagation constant β_d in the dielectric region, $h_1 = h_2 = 0.05$ in, $\varepsilon_d = 1$.

by about 1.85 GHz. The values of isolation and insertion loss at the circulation frequency are better in the two-disk case compared with the full height case.

Fig. 6 shows the variation of ferrite radius with circulation frequency for different disk heights. As the radius increases, the circulation frequency decreases, and for the same radius, the circulation frequency decreases with increase of disk heights.

When using two disks with unequal heights the variation of ferrite radius with circulation frequency is as shown in Fig. 7.

These two figures can be used in designing X-band E-plane circulators.

IV. Conclusions

The theory presented in this paper allows the determination of the propagation constants of the characteristic modes in each region of the central part of the junction

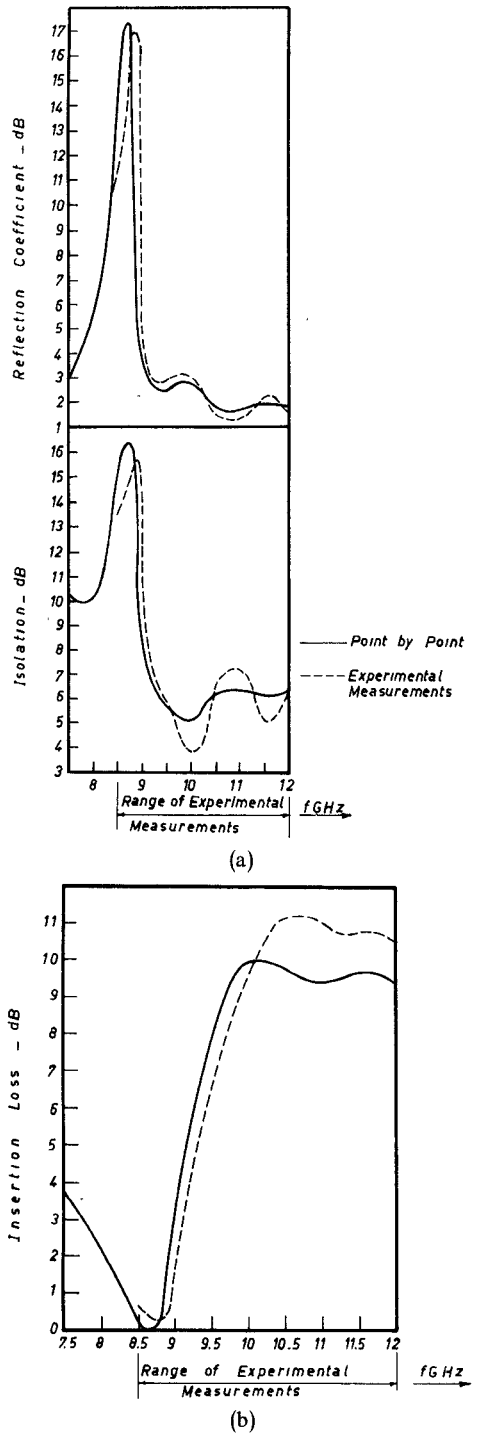

Fig. 5. Circulator characteristics for the two-disk circulator, $R = 0.1$ in, $h_1 = h_2 = 0.05$ in, $\varepsilon_d = 1$.

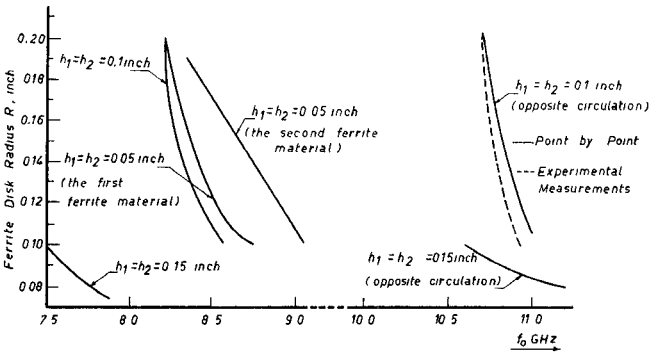

Fig. 6. Ferrite radius R versus frequency of circulation for different disk heights, $H_{dc} = 200$ Oe, material Y13A

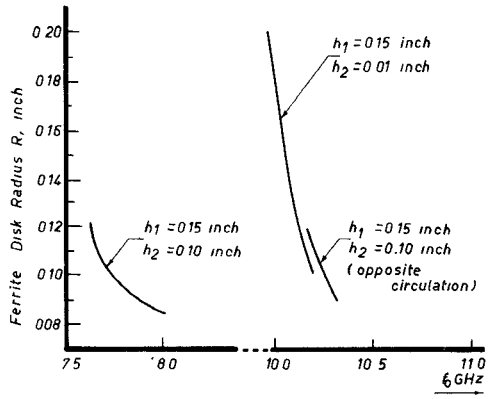

Fig. 7. Ferrite radius R versus frequency of circulation for disks with unequal heights, $H_{dc} = 200$ Oe, material Y13A.

which consists of two ferrite disks separated by a dielectric material. There are infinite values of the propagation constants at any frequency. However, not all of these modes are propagating. It is found that the propagation constants in the ferrite disks vary approximately linearly with frequency. The linearity increases by decreasing the ferrite disk height.

Circulator characteristics have been obtained numerically for different ferrite disks' heights and radii. The general shape of the circulator characteristic curves obtained by numerical technique and experimental measurements are found to be nearly the same, which verifies the theoretical treatment.

References

[1] R. F. Soohoo, *Theory and Application of Ferrite*. Englewood Cliffs, NJ: Prentice-Hall, 1960.

[2] B. Lax and K. J. Button, *Microwave Ferrites and Ferrimagnetics*. New York: Lincoln Laboratory Publications, McGraw-Hill, 1962.